

Three-body potential effects in the structure of fluid krypton

This article has been downloaded from IOPscience. Please scroll down to see the full text article.

1989 J. Phys.: Condens. Matter 1 7131

(<http://iopscience.iop.org/0953-8984/1/39/025>)

View [the table of contents for this issue](#), or go to the [journal homepage](#) for more

Download details:

IP Address: 171.66.16.96

The article was downloaded on 10/05/2010 at 20:17

Please note that [terms and conditions apply](#).

Three-body potential effects in the structure of fluid krypton

M Tau†, L Reatto‡, R Magli§, P A Egelstaff|| and F Barocchi¶

† Dipartimento di Fisica dell'Università, viale della Scienze, I43100 Parma, Italy

‡ Dipartimento di Fisica dell'Università, via Celoria 16, I20133 Milano, Italy

§ Dipartimento di Energetica, Università degli Studi, via di S Marta 3, I50139 Firenze, Italy

|| Department of Physics, University of Guelph, Guelph, Ontario, Canada

¶ Dipartimento di Fisica, Università degli Studi, largo E Fermi 2, I50125 Firenze, Italy

Received 28 March 1989

Abstract. The low-density expansion and a new integral equation have been used to calculate the pair correlation function and several related quantities for krypton, using realistic pair potentials and several models for the three-body potential: the Axilrod–Teller–Muto model, the multipolar model up to the triple quadrupole term and the Loubeyre model. The results are compared with experimental data in some detail. The models describe the three-body effects in correlation functions in a qualitative sense, but quantitative differences are observed, suggesting that shorter-ranged effects must also be included.

1. Introduction

Recent progress in the study of simple fluids has brought us to the point where the role of many-body forces must be discussed in detail. In this paper we shall employ several models to discuss the magnitude of effects involving three-body forces for states far from the critical point. Then we shall compare our results with experimental data on the static structure factor of krypton at room temperature and over a wide range of densities. This function is used because, through its dependence on wavevector, it allows a more sensitive test than that for bulk properties alone. In addition, as it is the Fourier transform of the pair correlation function, it has a simple physical interpretation.

We consider first the change in the pair correlation function at low densities for three different models of the three-body potential, and subsequently compare these predictions with experimental results. The models are the triple dipole (DDD) potential (Rice and Gray 1976), the multipole expansion (Rice and Gray 1976) up to the triple quadrupole term and a short-range model combined with the DDD term. Then we consider the same models at higher densities up to several times the critical density and show their variation with wavevector, and their comparison with experiment. We shall employ several methods of calculation. These include numerical integration of analytical formulae at low density, the use of a new modified hyper-netted chain (CRS-MHNC) theory over a range of densities including high densities, and in some instances molecular dynamics simulations. The krypton pair potentials due to Barker and to Aziz will be used also. A special effect beyond the simplest models of many-body effects is the

variation of the position of the principal peak in the structure factor with density. Predictions and observations of this effect will be presented as well.

The direct correlation function is often considered in the literature because it is simply related to the structure factor and has some simpler properties. Thus we display the full density and wavenumber dependence of our models and their comparison with experiment through this function. In addition, we plot the difference between the direct correlation functions (theoretical and experimental), as this difference is most closely related to the three-body potential term. Finally we make such comparisons for krypton at a lower temperature. Thus we shall use one of four presentations as most appropriate, namely the structure factor $S(k)$ itself, or the difference $\Delta S(k)$ between theory and experiment, or the direct correlation function $c(k)$ or finally the difference $\Delta c(k)$ between theory and experiment.

The object of this programme has been to combine the available theoretical and experimental results in a single comprehensive analysis of many-body problems in fluids. It is clear that accurate predictions for model potentials are available and that they do not agree wholly with the experimental data, although they do cover many of the general features adequately. Thus the present models need improvement in some cases to describe current data adequately, and this will be discussed in our conclusions. Our work suggests, also, that additional experimental data for the isothermal compressibility and for the structure factor would be worth while.

2. Model potentials

We have used for $u_2(1, 2)$ the empirical pair potentials derived by Barker *et al* (1974) and by Aziz (1979) or Aziz *et al* (1986). For the three-body potential we will assume three different models:

(a) The 'long-range' (Axilrod and Teller 1943, Muto 1943) triple dipole, given by

$$u_3(1, 2, 3) = \frac{\nu(1 + 3 \cos \Phi_1 \cos \Phi_2 \cos \Phi_3)}{r_{12}^3 r_{23}^3 r_{13}^3} \quad (1)$$

where $\nu = 220.4 \times 10^{-84}$ erg cm⁹.

(b) The 'long-range' potential with all the terms of the multipolar expansion up to the triple quadrupole given by Doran and Zucker (1971) and Bell (1970):

$$u_3(1, 2, 3) = Z(DDD)_3 W(DDD)_3 + Z(DDQ)_3 W(DDQ)_3 \\ + Z(DQQ)_3 W(DQQ)_3 + Z(QQQ)_3 W(QQQ)_3 \quad (2)$$

with

$$W(DDD)_3 = \frac{1 + 3 \cos \Phi_1 \cos \Phi_2 \cos \Phi_3}{3r_{12}^3 r_{23}^3 r_{13}^3}$$

$$W(DDQ)_3 = \frac{3}{16r_{12}^3 r_{23}^4 r_{31}^4} [9 \cos \Phi_3 - 25 \cos \Phi_3 + 6 \cos(\Phi_1 - \Phi_2) - (3 + 5 \cos 2\Phi_3)]$$

Table 1. Interaction constants for a triplet of Kr atoms (from Doran and Zucker 1971)—see equation (2) in the text.

$$\begin{aligned} Z(\text{DDD})_3 &= 73.47 \times 10^{-84} \text{ erg cm}^9 \\ Z(\text{DDQ})_3 &= 8097 \times 10^{-102} \text{ erg cm}^{11} \\ Z(\text{DQQ})_3 &= 8761 \times 10^{-118} \text{ erg cm}^{13} \\ Z(\text{QQQ})_3 &= 94926 \times 10^{-135} \text{ erg cm}^{15} \end{aligned}$$

Table 2. Values of the constants in the Loubeyre (1987) formula—see equation (3) in the text.

$$\begin{aligned} \nu &= 220.4 \times 10^{-84} \text{ erg cm}^9 \\ A &= 7.4866 \times 10^{-8} \text{ erg} \\ \alpha &= 1.546 \times 10^8 \text{ cm}^{-1} \end{aligned}$$

$$\begin{aligned} W(\text{DQQ})_3 &= \frac{15}{64r_{12}^5 r_{23}^4 r_{13}^4} [3(\cos \Phi_3 + 5 \cos 3\Phi_3) \\ &\quad + 20 \cos(\Phi_1 - \Phi_2)(1 - 3 \cos 2\Phi_3) + 70 \cos 2(\Phi_1 - \Phi_2) \cos \Phi_3] \\ W(\text{QQQ})_3 &= \frac{15}{128r_{12}^5 r_{23}^5 r_{13}^5} \{-27 + 220 \cos \Phi_1 \cos \Phi_2 \cos \Phi_3 \\ &\quad + 490 \cos 2\Phi_1 \cos 2\Phi_2 \cos 2\Phi_3 \\ &\quad + 175[\cos 2(\Phi_1 - \Phi_2) + \cos 2(\Phi_2 - \Phi_3) + \cos 2(\Phi_3 - \Phi_1)]\}. \end{aligned}$$

The values for the Z numerical factors in equation (15) are given in table 1.

(c) The 'short-range' exponential potential plus the Axilrod–Teller triple dipole recently used by Loubeyre (1987), and given by

$$\begin{aligned} u_3(1, 2, 3) &= \{\nu(r_{12}^3 r_{23}^3 r_{13}^3)^{-1} - A \exp[-\alpha(r_{12} + r_{23} + r_{13})]\} \\ &\quad \times (1 + 3 \cos \Phi_1 \cos \Phi_2 \cos \Phi_3). \end{aligned} \quad (3)$$

In the previous formulae the Φ_i are the angles of the triangle formed by r_i , $i = 1, 2, 3$. The values of the numerical constants ν , Z , A and α are given in table 2.

The first potential is often employed in the literature for the representation of three-body irreducible forces in fluids; the second one is a refinement of the first one, which is useful for example for the description of the third virial coefficient of gases (Barker 1986); while the third model has been found to give a good account of very high-density thermodynamic properties of noble gases and is also the first model that explicitly takes into account short-range three-body irreducible forces.

3. The low-density region

3.1. Low-density theory

Let us consider a low-density gas composed of N atoms contained in a volume V ; if the total interaction energy $U(1, \dots, N)$ can be cluster-expanded as

$$U(1, \dots, N) = \sum_{i>j} u_2(i, j) + \sum_{i>j>k} u_3(i, j, k) + \dots \quad (4)$$

where $u_2(i, j)$ is the interaction potential of the isolated pair (i, j) and $u_3(i, j, k)$ is the

irreducible part of the potential of the isolated triplet (i, j, k), then the pair distribution function $g(r_{12})$, referred to a generic pair (1, 2), can be series-expanded as a function of the density n , i.e. (Rice and Gray 1976)

$$g(r_{12}) = g_0(r_{12}) + ng_1(r_{12}) + O(n^2) \quad (5)$$

where

$$g_0(r_{12}) = \exp[-u_2(1, 2)/k_B T] \quad (6)$$

and

$$g_1(r_{12}) = g_1^{(2)}(r_{12}) + g_1^{(3)}(r_{12}) \quad (7)$$

$$g_1^{(2)}(r_{12}) = g_0(r_{12}) \int f(r_{13})f(|\mathbf{r}_{12} - \mathbf{r}_{13}|) d\mathbf{r}_{13} \quad (8)$$

$$g_1^{(3)}(r_{12}) = g_0(r_{12}) \int g_0(r_{13})g_0(|\mathbf{r}_{12} - \mathbf{r}_{13}|)\{\exp[-u_3(1, 2, 3)/k_B T] - 1\} d\mathbf{r}_{13}. \quad (9)$$

Here, atoms 1, 2 and 3 describe a triangle whose sides are r_{12} , r_{13} and r_{23} respectively. In the last equations $f(r_{12}) = g_0(r_{12}) - 1$ is the Mayer function and $g_1^{(2)}(r_{12})$ indicates the part of $g_1(r_{12})$ that depends only on the two-body potential while $g_1^{(3)}(r_{12})$ depends also on the three-body one.

It is worth mentioning that the series expansion with respect to the density n has a different radius of convergence n_0 for each value of r_{12} , with n_0 decreasing to zero as $r_{12} \rightarrow \infty$, therefore requiring some care. In particular one should, in principle, know at least the size of the n^2 term in equation (5) before approximating the sum of equation (5) by the first two terms. Here we will not discuss the n^2 term of equation (2) because its calculation even for a pure two-body potential is cumbersome.

The neutron scattering structure factor $S(k)$ is related to the pair distribution function by a Fourier transformation, i.e.

$$S(k) = 1 + n \int [g(r_{12}) - 1] \exp(-i\mathbf{k} \cdot \mathbf{r}_{12}) d\mathbf{r}_{12}. \quad (10)$$

Therefore from equations (2) and (7) also $S(k)$ can be represented as a series expansion with respect to the density n . In particular it is convenient to refer to the function $H(k) = [S(k) - 1]/n$, and the Ornstein-Zernike direct correlation function $c(k) = H(k)/S(k)$. From equations (5) and (10) we have

$$\begin{aligned} c(k) &= c_0(k) + nc_1(k) + O(n^2) \\ H(k) &= H_0(k) + nH_1(k) + O(n^2) \end{aligned} \quad (11)$$

where

$$H_0(k) = \int [g_0(r_{12}) - 1] \exp(i\mathbf{k} \cdot \mathbf{r}_{12}) d\mathbf{r}_{12} = c_0(k) \quad (12)$$

and

$$H_1(k) = \int g_1(r_{12}) \exp(i\mathbf{k} \cdot \mathbf{r}_{12}) d\mathbf{r}_{12}. \quad (13)$$

From equations (7) and (13) we also have

$$\begin{aligned}
 H_1(k) &= H_1^{(2)}(k) + H_1^{(3)}(k) \\
 c_1(k) &= c_1^{(2)}(k) + c_1^{(3)}(k)
 \end{aligned}
 \tag{14}$$

with

$$\begin{aligned}
 H_1^{(2)}(k) &= \int g_1^{(2)}(r_{12}) \exp(i\mathbf{k} \cdot \mathbf{r}_{12}) \, d\mathbf{r}_{12} = [H_0(k)]^2 + c_1^{(2)}(k) \\
 c_1^{(2)}(k) &= H_1^{(2)}(k) - [H_0(k)]^2 = \iint f(r_{12})f(r_{13})f(|\mathbf{r}_{12} - \mathbf{r}_{13}|) \\
 &\quad \times \exp(i\mathbf{k} \cdot \mathbf{r}_{12}) \, d\mathbf{r}_{12} \, d\mathbf{r}_{13}
 \end{aligned}
 \tag{15}$$

and

$$H_1^{(3)}(k) = \int g_1^{(3)}(r_{12}) \exp(i\mathbf{k} \cdot \mathbf{r}_{12}) \, d\mathbf{r}_{12} = c_1^{(3)}(k).
 \tag{16}$$

In a similar way to equation (5), the series expansion (11) has a different radius of convergence n'_0 for each k value, with n'_0 becoming smaller when $k \rightarrow 0$. Equations (6) to (9) offer the possibility of calculating the first two terms of the series expansion of $g(r_{12})$ and in particular the two parts of $g_1(r_{12})$ which depend on the two-body potential and also on the three-body one respectively. In order to understand whether it is possible to measure the part of $g(r_{12})$ related to the three-body potential, it is important to calculate the relative size of $g_0(r_{12})$ and $ng_1(r_{12})$ and of $g_1^{(3)}(r_{12})$ compared to $g_1^{(2)}(r_{12})$. The computer calculation of the integrals in equations (8) and (9) gives this possibility once a model is chosen for the two-body potential $u_2(1, 2)$ and the three-body potential $u_3(1, 2, 3)$. Such calculations using the Barker potential for u_2 and the Axilrod–Teller potential for u_3 were reported by Teitsma and Egelstaff (1980) and by Egelstaff *et al* (1980). A computer program that evaluates the integrals (7) to (9) and their Fourier transforms has been reported by Ram *et al* (1982), and some examples given. We have developed our own program for the computation of these quantities. In addition we have also deduced $c_0(k)$, $c_1^{(2)}(k)$ and $c_1^{(3)}(k)$ from the solution at very low density of the integral equation, which is discussed in the next section and which is exact to linear order in the density.

3.2. Low-density results

The integrals in equations (8) and (9) were evaluated with a careful analysis of their convergence. Figure 1 gives the behaviour of the contribution of g_1 and $g_1^{(3)}$ for the three different three-body potentials we have used in the calculations when u_2 is the Barker potential. The introduction of other multipolar contributions in u_3 , besides the triple dipole one, slightly increases the negative peak of $g_1^{(3)}$ while the introduction of the exponential part of Loubeyre drastically decreases the negative peak of $g_1^{(3)}$ by approximately a factor 2 and makes the contribution less soft than in the other cases, shifting slightly its effective hard core.

We have calculated also, by means of a simple Fourier transform, the correction to the low-density structure factor, i.e. the functions $H_1^{(2)}(k)$ and $H_1^{(3)}(k)$. For $H_1^{(2)}$ and $H_1^{(3)}$ the different behaviour is more evident at low k -values where it is mainly determined by the opposite value and different size of the zero moments of $g_1^{(2)}$ and $g_1^{(3)}$ respectively. Figure 2 shows $c_1^{(3)}$ (or $H_1^{(3)}$) in the three cases at $T = 297$ K. Here we see that when the

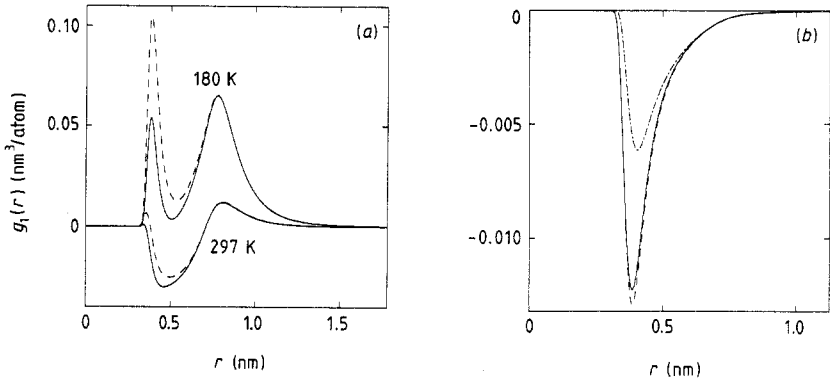


Figure 1. (a) The first density corrections $g_1^{(2)}(r)$ (broken curves) and $g_1(r) = g_1^{(2)}(r) + g_1^{(3)}(r)$ (full curves) to $g(r)$ for the Barker plus DDD interaction at two temperatures. (b) The three-body contribution $g_1^{(3)}(r)$ at $T = 297$ K for the Barker u_2 and different models of u_3 : DDD (full curve), DDD + DDDQ + DQQ + QQQ (broken curve) and Loubeyre model (chain curve).

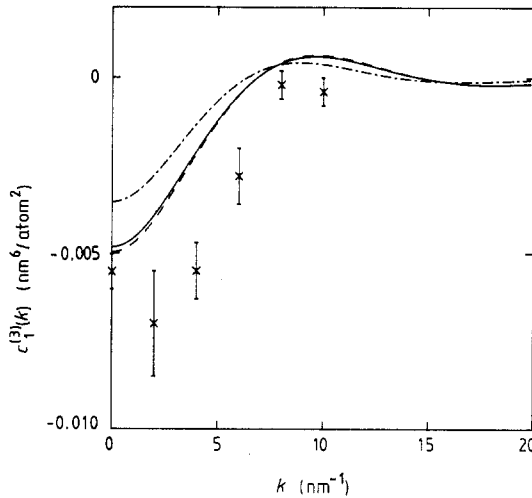


Figure 2. Three-body contribution $c_1^{(3)}(k)$ to the first density correction to $c(k)$ at $T = 297$ K. Symbols are as in figure 1(b). Crosses represent an estimation of $c_1^{(3)}(k)$ from $c(k)_{\text{pair}} - c(k)_{\text{expt}}$ as discussed in the text.

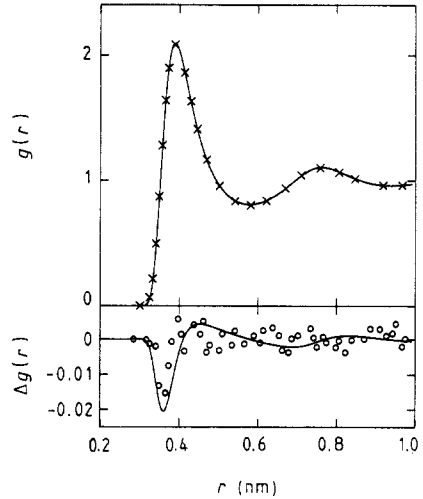


Figure 3. The function $g(r)$ for krypton at $T = 297$ K and $n = 13.84$ atoms/ nm^3 for HFGKR pair potential (Aziz 1979) with three-body DDD interaction: simulation (Levesque and Weis 1988) (\times); optimised CRS-MHNC (—). Difference $\Delta g(r) = g^{(3)} - g^{(2)}$ of the radial distribution function with and without the DDD interaction: simulation (\circ); optimised CRS-MHNC (—).

full multipolar potential is used instead of the Axilrod–Teller–Muto triple dipole one only a small change in $c_1^{(3)}$ is obtained. The Loubeyre form decreases the amplitude of $c_1^{(3)}$ with a very slight shift in k to smaller value. In table 3 we give the value of c_0 , $c_1^{(2)}$ and $c_1^{(3)}$ for selected values of k both for the Aziz (1979) and for the Barker *et al* (1974) pair potential and for the triple dipole three-body interaction. One can see that $c_1^{(2)}$ and $c_1^{(3)}$ are very insensitive to the chosen form of the pair interaction for all k -values, the

Table 3. Coefficients of the low-density expansion (11) and (14) of $c(k)$ for the Aziz (1979) (A) and for the Barker *et al* (1974) (B) pair interactions, together with the triple dipole three-body interaction. For $k > 10 \text{ nm}^{-1}$ we give only the Aziz result, the Barker one being almost the same. The experimental data (E) have been obtained from a fit as discussed in the text and $c_1^{(3)}$ has been obtained by subtracting the Barker $c_1^{(2)}$ from c_1 .

k (nm^{-1})		$c_0(k)$ (nm^3/atom)	$c_1^{(2)} \times 10^2$ ($\text{nm}^6/\text{atom}^2$)	$c_1^{(3)} \times 10^2$ ($\text{nm}^6/\text{atom}^2$)	$(c_1 = c_1^{(2)} + c_1^{(3)}) \times 10^2$ ($\text{nm}^6/\text{atom}^2$)
0	A	0.1737	-1.387	-0.475	-1.862
	B	0.1680	-1.376	-0.479	-1.855
	E	0.168 ± 0.007		(-0.55)	-1.93 ± 0.05
1	A	0.1565	-1.367	-0.453	-1.820
	B	0.1517	-1.356	-0.457	-1.813
2	A	0.1145	-1.307	-0.392	-1.699
	B	0.1118	-1.296	-0.395	-1.691
	E			(-0.70)	-2.00 ± 0.15
4	A	0.0065	-1.092	-0.210	-1.302
	B	0.0074	-1.080	-0.212	-1.293
	E			(-0.55)	-1.63 ± 0.08
6	A	-0.0767	-0.815	-0.046	-0.861
	B	-0.0751	-0.806	-0.047	-0.853
	E			(-0.27)	-1.08 ± 0.08
8	A	-0.1053	-0.568	0.042	-0.527
	B	-0.1046	-0.561	0.041	-0.519
	E			(-0.02)	-0.58 ± 0.04
10	A	-0.0844	-0.398	0.060	-0.338
	B	-0.0847	-0.392	0.060	-0.332
	E			(-0.04)	-0.43 ± 0.04
12	A	-0.0387	-0.287	0.038	-0.249
14	A	0.0051	-0.200	0.008	-0.192
16	A	0.0298	-0.120	-0.013	-0.133
18	A	0.0319	-0.053	-0.020	-0.074
20	A	0.0184	-0.011	-0.016	-0.027
22	A	0.0006	0.004	-0.005	-0.001
24	A	-0.0119	0.001	0.005	0.006
26	A	-0.0151	-0.010	0.010	0.000

difference between the Aziz and the Barker potentials being well below 1%. This is not so for $c_0(k)$ ($=H_0(k)$) at small k ; for instance at $k = 0$ there is a 3.5% difference between the two pair potentials. The difference is even more pronounced in $H_1^{(2)}$ because it depends on $(H_0)^2$ (see equation (15)); for instance we find $H_1^{(2)} = 0.0163 \text{ nm}^6/\text{atoms}^2$ for Aziz and $H_1^{(2)} = 0.0145 \text{ nm}^6/\text{atoms}^2$ for Barker. Use of the later Aziz potential (Aziz *et al* 1986) leads to only a negligible change in c_0 and c_1 and in what follows we have used the former one (Aziz 1979). We find that our value for $c_1^{(3)}(k)$ differs from the one computed with Cummings' program (Ram *et al* 1982). Since we have agreement between the $c_1^{(3)}(k)$ computed in two completely independent ways, directly from equation (16) and from the integral equation, we believe that our results are correct.

In figure 2 and in table 3 we show also results obtained from the experimental data for the equation of state (Trappeniers *et al* 1966, Michels *et al* 1960) and the structure factor (Teitsma and Egelstaff 1980). Owing to the sensitivity of H_0 and H_1 on the precise form of the pair potential, it is preferable to analyse the data in terms of the c function. From the experimental equation-of-state data we estimate $c(0) = [1 - (\partial p/$

$\partial n)_T(k_B T)^{-1}/n$ by taking the finite-difference ratios from 0.6 to 16.5 atoms/nm³, and from a best quadratic fit in n of the data below 3 atoms/nm³ we obtain $c_0(0)$ and $c_1(0)$. The value of $c_1(0)$ is in agreement with the theoretical value within the experimental error when the triple dipole interaction is included and no preference can be given either to the Aziz potential or to the Barker one. The experimental $c_0(0)$ is close to the Barker value and deviates from the Aziz one. This is because this last pair potential has used as fitting data, in addition to other quantities, second virial coefficient data that are larger than the value deduced from the Trappeniers *et al* (1966) data roughly in the same proportion of the Aziz and of the Barker value for $c_0(0)$. On the other hand the later Aziz potential (Aziz *et al* 1986), which gives essentially the same value for $c_1(0)$, does not make use of virial data for the determination of u_2 . This suggests that it might be worth while repeating the measurements at the lowest densities.

In figure 2 the 'experimental' value of $c_1^{(3)}(0)$ is obtained by taking the difference between the experimental $c_1(0)$ and the Barker value for $c_1^{(2)}(0)$. The value of $c_1^{(3)}(0)$ is in good agreement with the triple dipole model, in particular when the higher multipolar terms are also included (figure 2). The Loubeyre model gives a too small value for $c_1^{(3)}(0)$. Also shown in figure 2 is an estimation of $c_1^{(3)}(k)$. This quantity was first obtained by Teitsma and Egelstaff (1980) from the measured $c(k)$ as the difference between the slopes with respect to n of the best linear fit of the measured $c(k)$ and of the computed $c_1^{(2)}(k)$ for $n < 6$. Egelstaff *et al* (1980) made Monte Carlo simulations of krypton at several densities at 297 K (which were later repeated and extended by Ram and Egelstaff (1984)), and showed that the range of density over which the data on $c(k)$ were linear varied with k and with the accuracy of the data being large at high k and falling significantly at lower k . For example for $k = 6 \text{ nm}^{-1}$ and $S(k)$ determined to $\sim 1\%$, the linear range was 5 atoms/nm³. A revised estimate of $c_1^{(3)}(k)$ was not published, however. As explained in the next section we have made calculations for the experimental densities of Teitsma and Egelstaff (1980) using the CRS-MHNC equation (Foiles *et al* 1984), and our $S(k)$ data agree with the above Monte Carlo (MC) data typically to $\sim 1\%$. Since this is within the errors on these MC data, we prefer our CRS-MHNC results and using them have re-evaluated the difference; using only the linear range in n we have estimated $c_1^{(3)}(k)$ from the best linear fit of $c(k)_{\text{pair}} - c(k)_{\text{expt}}$ by using the Barker pair potential. These re-evaluated data are shown in figure 2 and in table 3, and they are shifted from the data of Teitsma and Egelstaff (1980) by amounts comparable to the errors. Nevertheless the new evaluation still shows important differences from the multipole model for $k \neq 0$.

We also note that the quantity $c(k)_{\text{pair}} - c(k)_{\text{expt}}$ should extrapolate to zero as $n \rightarrow 0$, if the true pair potential had been used in the calculations. As pointed out by Egelstaff *et al* (1980), this rule is not satisfied exactly, suggesting that some subtle modification of the Aziz and Barker pair potentials is needed. It seems likely that such a modification will not change the estimated $c_1^{(3)}$ by a significant amount, and hence not materially alter our conclusion that either some additional terms are needed in the three-body potentials, or the experimental errors are significantly larger than quoted.

4. From low to high density

4.1. Integral equation

The computation of $H(k)$ from the virial expansion beyond the linear order in density is cumbersome and of limited use, and one has to resort either to simulation or to the

integral equation method for $g(r)$. The first advantage of the integral equation is that the numerical effort is much reduced compared to simulation so that one can easily explore different forms for the inter-atomic interaction and find small changes in the structure, which in simulation are obscured by the statistical noise. The second advantage is the absence of a size effect typical of simulation, with the resulting uncertainty in deducing the structure factor in particular at small k . Therefore if the accuracy of the integral equation is comparable to the estimated precision of the experimental data on $S(k)$ it is actually advantageous to use the result of the integral equation for comparison with the experimental data in order to get information on the inter-atomic potential. With the development by Reatto and Tau (1987) of accurate integral equations for $g(r)$ when three-body forces are present we believe that presently this is the case for simple one-component fluids as a result of detailed comparison (Celi *et al* 1989) with accurate simulation results in a few benchmark cases, both in the case of two-body forces and in the case where the three-body DDD interaction is also present. Below we present some additional results in this respect.

Here we are going to use a cross-over hyper-netted chain (CRS-MHNC) equation (Foiles *et al* 1984) as generalised (Reatto and Tau 1987) when three-body forces are present. The pair distribution function is related to the two- and three-body potential by the relation

$$g(r_{12}) = \exp[-\beta u_2(r_{12}) + h(r_{12}) - c(r_{12}) + C(r_{12}) + E_{\text{CRS}}(r_{12})] \quad (17)$$

where $h(r) = g(r) - 1$, $c(r)$ is the direct correlation function defined by the Ornstein-Zernike (OZ) relation

$$h(r_{12}) = c(r_{12}) + n \int d^3 r_3 c(r_{13}) h(r_{32}) \quad (18)$$

the three-body vertex is given by

$$C(r_{12}) = n \int d^3 r_3 g(r_{13}) g(r_{23}) \{ \exp[-\beta u^{(3)}(1, 2)] - 1 \} \quad (19)$$

and the cross-over model bridge function reads

$$E_{\text{CRS}}(r) = [1 - l(r)] E_{\text{HS}}(r; d) + l(r) [-h(r) + \ln g(r)]. \quad (20)$$

Here $l(r)$ is an empirical cross-over function, which vanishes in the core region and is unity at large distance. We have used the form (Reatto and Tau 1987)

$$l(r) = \begin{cases} 0 & \text{for } r < R - \omega \\ \frac{1}{2} [1 + \tanh\{(r - R)/[\omega^2 - (r - R)^2]^{1/2}\}] & \text{for } R - \omega < r < R + \omega \\ 1 & \text{for } r > R + \omega. \end{cases} \quad (21)$$

In this way for $r < R - \omega$ the bridge function is approximated by the one of hard spheres E_{HS} and for $r > R + \omega$ $E_{\text{CRS}}(r)$ has the functional form corresponding to the mean spherical approximation for which $c(r) = -\beta u_2(r)$. If only two-body forces are present one simply drops the $C(r)$ terms in equation (17). The model bridge function (20) depends on three parameters, the hard-sphere diameter d and the cross-over parameters R and ω . When only two-body forces are present one can develop (Celi *et*

al 1989) suitable Lado's (1982) criteria which determine these parameters, the one derived from variation of d being

$$\int d^3r [g(r) - g_{\text{HS}}(r; d)] [1 - l(r)] \frac{\partial E_{\text{HS}}(r; d)}{\partial d} = 0 \quad (22)$$

and those derived from variation of R and ω reading

$$\int d^3r \{ [g(r) - g_{\text{HS}}(r)] E_{\text{HS}}(r) + [(g(r))^2 - (g_{\text{HS}}(r))^2] / 2 - [g(r) \ln g(r) - g_{\text{HS}}(r) \ln g_{\text{HS}}(r)] \} \frac{\partial l(r)}{\partial R} = 0 \quad (23)$$

$$\int d^3r \{ [g(r) - g_{\text{HS}}(r)] E_{\text{HS}}(r) + [(g(r))^2 - (g_{\text{HS}}(r))^2] / 2 - [g(r) \ln g(r) - g_{\text{HS}}(r) \ln g_{\text{HS}}(r)] \} \frac{\partial l(r)}{\partial \omega} = 0. \quad (24)$$

In the present computation we have used for E_{HS} the hard-sphere bridge function deduced from the Verlet and Weis (1972) parametrisation of g_{HS} with the extension of Henderson and Grundke (1975) inside the core. When u_3 is present we use the same cross-over parameters as determined for the two-body forces. Then equations (17)–(24) form a closed set of equations, which are solved by a standard numerical method (Reatto and Tau 1987). The exponential function in (19) has been expanded to linear order in $u^{(3)}$.

As an example of the tests we have performed on the CRS-MHNC equation we consider the result of a recent accurate simulation (Levesque and Weis 1988) for dense Kr gas at $T = 297$ K and $n = 13.84$ atoms/nm³. In this simulation as pair potential the HFGKR potential by Aziz (1979), which has a well depth $\varepsilon/k_{\text{B}} = 199.9$ K and minimum of u_2 at $r_m = 0.4012$ nm, was truncated at $L/2 = 0.992$ nm and then used without and with the three-body DDD interaction (1). For the purpose of comparison we have solved the CRS-MHNC equation with these truncated potentials (the optimised parameters of the bridge function turn out to be $d = 0.8751 r_m$, $R = 1.75 r_m$ and $w = 0.67 r_m$) and from figure 3 one can see that the computed $g(r)$ is almost indistinguishable from simulation, the typical deviations in $g(r)$ being of the order of ± 0.01 , just twice the estimated statistical error of the simulation. In the same figure we show the difference $\Delta g = g^{(3)} - g^{(2)}$ between the pair distribution function when the DDD interaction is present and when it is absent. The effect of this three-body interaction is quite small ($< 0.5\%$) and only in the core region is it outside the statistical noise of simulation ($\sim 1.5\%$). The integral equation reproduces this effect quite well. Additional comparisons with simulation (Celi et al 1989) indicate that the effect of the DDD interaction is reproduced with a similar accuracy also in the triple-point region. However, in the triple-point region the typical deviation in $g(r)$ between theory and simulation increases at the level of ± 0.03 (Celi et al 1989) but the origin of this deviation is mainly due to the way the two-body potential is treated. Also we have computed $S(k)$ for the 15 densities at 297 K used by Teitsma and Egelstaff (1980), and compared these data for $2 \leq k \leq 10$ nm⁻¹ with the Monte Carlo simulations of Ram and Egelstaff (1984) and found agreement to better than 1%, which is within the error on the simulations.

If we exclude the immediate neighbourhood of the critical point, where critical fluctuations become important, the integral equation is even more accurate at lower

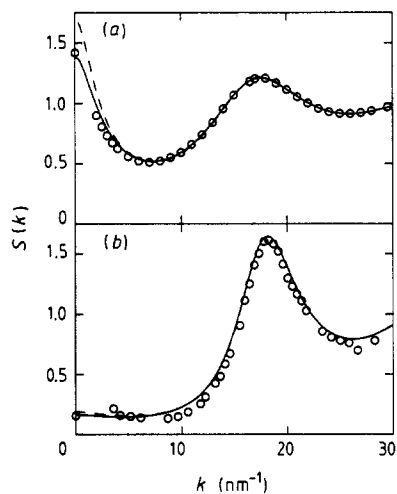


Figure 4. The function $S(k)$ for krypton at $T = 297$ K and (a) $n = 6.19$ and (b) $n = 13.84$ atoms/nm³. Experimental data (Teitsma and Egelstaff 1980, Egelstaff *et al* 1983) (\circ) and optimised CRS-MHNC for (Barker *et al* 1974) pair interaction with and without DDD interaction: two plus three-body (—); two-body (---).

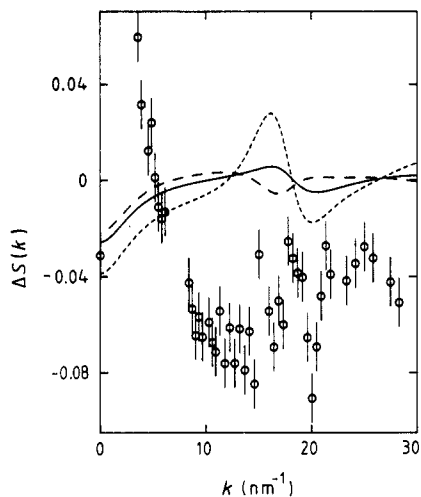


Figure 5. Difference $\Delta S(k) = S^{(3)}(k) - S^{(2)}(k)$ between the structure factor with and without the three-body interaction with the optimised CRS-MHNC equation for krypton at $T = 297$ K and $n = 13.84$ atoms/nm³: DDD (—); Loubyere model with the increased strength $\nu = 298.2 \times 10^{-84}$ erg cm⁹; QOO with the increased strength $Z_3 = 625.4 \times 10^{-130}$ erg cm¹⁵ (---). Circles represent the difference between experiment and $S^{(2)}$, using the Aziz u_2 .

densities and it is exact at linear order in density. We conclude that the triplet CRS-MHNC equation can be used at the level of 1–2% to test the effects of a three-body interaction. For only the two-body interaction the equation is very accurate for temperatures above the critical one, and small deviations only occur in the triple-point region.

4.2. Room-temperature isotherm

Extensive measurements (Teitsma and Egelstaff 1980, Egelstaff *et al* 1983) of the structure factor by neutron scattering along the room-temperature isotherm have already been used in order to test models for the inter-atomic interaction in Kr. Here we do the same but on the basis of the integral equation results and not of simulation so that we do not have to worry about size effects and we can study the small- k behaviour. We also test other forms for the three-body interaction.

At low density the agreement between theory and experiment is rather good and we shall return to this below. Starting from a density of order 6 atoms/nm³ some sizable deviations set in and in figure 4 we give the results for $S(k)$ at $n = 6.19$ and 13.84 atoms/nm³. Here and in all other figures the experimental value at $k = 0$ is deduced from the thermodynamic measurements (Trappeniers *et al* 1966, Michels *et al* 1960). The estimated error (Teitsma and Egelstaff 1980) of the neutron scattering measurements at $n = 6.19$ is below the size of the symbols. The theoretical results differ slightly from the ones reported previously (Reatto and Tau 1987) because now the cross-over parameters are fully optimised. The $k = 0$ value is well reproduced by theory when the

DDD interaction is included and at larger k the effect of the three-body interaction is very small. At the smaller density of figure 4 the deviation between theory and neutron data is significant only below $k \approx 5 \text{ nm}^{-1}$ but at the larger density the deviation is present over most of the measured k -range. This is shown more clearly in figure 5, where the difference $\Delta S(k)$ between the experimental data at 13.84 atoms/nm^3 and the theoretical result for the Aziz potential is shown. If this potential were the exact two-body interaction, this difference would be the effect of many-body forces in krypton at this high density. In the same figure we plot the theoretical $\Delta S(k)$ for some models of the three-body interaction. For the correct model of many-body forces this $\Delta S(k)$ should coincide with the circles. It is clear that the DDD three-body interaction is reasonable for $k = 0$ but it is inadequate at finite k .

We have considered two other forms for the three-body interaction. The first is the modified DDD form (3), but this gives an effect on $S(k)$ even smaller than the DDD form and the compressibility is not correct (this is not shown in the figure). In order to obviate this we have increased the strength ν from the value of table 2 to the value $\nu = 298.2 \times 10^{-84} \text{ erg cm}^9$ so that the third virial coefficient for the equation of state at $T = 297 \text{ K}$ has the same value as the pure DDD form. The effect on $S(k)$ remains small as shown in figure 5. We have also modified the DDD form (1) in a different way by an exponential damping of u_3 at short distance, as suggested by Bulski and Chalasinski (1987), but also in this case the effect on $S(k)$ remains small. All these forms of u_3 have the same angular dependence of the DDD form. Since a two-body quadrupolar interaction has a stronger effect on the structure (Patey and Valleau 1976) than the dipolar one, we have considered a pure triple quadrupole interaction, i.e. $u_3 = Z(\text{QQQ})_3 W(\text{QQQ})_3$ (see equation (2)), with an increased strength $Z(\text{QQQ})_3 = 62545.9 \times 10^{-132} \text{ erg cm}^{15}$ such that it gives the correct value of the third virial coefficient at $T = 297 \text{ K}$. We see from figure 5 that this u_3 is more efficient in modifying $S(k)$ but the effect is very different from that needed to bring agreement with experiment.

None of these models for u_3 are able to explain the observed $S(k)$ at high density. The magnitude of the observed deviations is so large that we do not believe it is likely that its origin is due to some defect of the model pair interaction like the Aziz or the Barker one, but it should be due to additional many-body forces unless there is some additional source of error in the experimental data. In particular we have considered the possibility that the calibration of the absolute scale for neutron scattering at the higher densities (Egelstaff *et al* 1983) was slightly in error. A change of this scale can improve the agreement with the theoretical result in a restricted region of k -values, for instance in the region of the main maximum of $S(k)$, but it is not possible to obtain agreement over the full k -range.

A characteristic feature of $S(k)$ is the position k_m of the main maximum of $S(k)$ and this is plotted in figure 6 as function of density. The three-body DDD interaction displaces k_m slightly to a smaller value as a consequence of a small outward displacement of the first shell of neighbours. The theory is in good agreement with the result of simulation using the DDD model. In fact at the density 13.84 atoms/nm^3 we find $k_m = 18.19 \text{ nm}^{-1}$ and from simulation (Levesque and Weis 1988) one gets $k_m = 18.17 \text{ nm}^{-1}$. At small density the experimental data are not meaningful owing to the large uncertainty in the determination of k_m because the maximum is very broad, and there is agreement (within large error) in the intermediate-density region. But deviations are present at high density, which may be genuine and indicate that additional many-body forces induce an outward displacement of the first shell of neighbours of order of 1%.

A useful way of presenting the large number of data in a way that puts more in evidence the effects of the inter-atomic interaction is by a plot of $c(k)$ as a function of

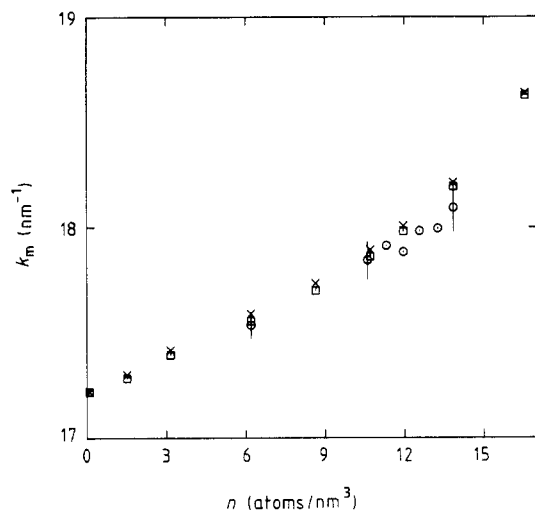


Figure 6. Position of the maximum of $S(k)$ for krypton at $T = 297$ K as a function of density: experiments (Teitsma and Egelstaff 1980, Egelstaff *et al* 1983) (\circ); optimised CRS-MHNC for Barker pair interaction with (\square) and without (\times) the DDD interaction. The Aziz u_2 gives essentially the same results.

density at fixed k . This function is simply given by $c(k) = [1 - S^{-1}(k)]/n$. The mathematical form of this function makes the errors large at small and large n . We extend in figure 7 the presentation of Teitsma and Egelstaff (1980) to larger densities. In this figure we show the actual $c(k)$ versus n for several values of k for the Barker potential with and without the three-body DDD interaction. Apart from $k = 0$ the Aziz u_2 gives essentially indistinguishable results and we plot the results for Barker u_2 because with this potential we have performed a more extended series of computations. At $k = 0$ it is important to include the three-body potential in order to get close to experiment. The remaining discrepancies for $k = 0$ are rather small, becoming appreciable only at the highest densities. Larger differences are visible at higher k and these increase with increasing density as expected. Above about 6 atoms/nm³ the deviation between theory and experiment increases rapidly with density and it is well outside the joint uncertainty of the theory and of experiment, and the discrepancy is present for all k -values. The difference $\Delta c(k)$ between the pair result for $c(k)$ and the experimental result as function of n shows the effect of many-body forces if the pair interaction is the exact one. In figure 7(b), $c(k)$ deduced from simulation with the DDD interaction and the Aziz u_2 at $n = 13.84$ atoms/nm³ is also shown.

We consider now more closely the effect of many-body forces on $c(k)$. The most appropriate comparison with experiment is for $k = 0$, partly because these data are an integral over all space (and so at low densities should involve mainly the long-range interactions) and partly because the experimental results are more accurate than at higher k . In the first place we show as a full curve in figure 8 the difference $\Delta_{\text{th}}c(0)$ between the pair model result and the result obtained when also the three-body DDD interaction is included. The CRS-MHNC method has been used and in figure 8 we show the result for the Barker interaction. We have performed the same computation with the Aziz potential and obtained results essentially indistinguishable from the Barker ones for $\Delta_{\text{th}}c(0)$. Therefore we conclude that $\Delta_{\text{th}}c(0)$ is essentially independent of which pair interaction is used and this extends up to freezing density, an observation we have already made on the basis of the virial expansion results.

Then we plot in figure 8 the difference $\Delta_{\text{exp}}c(0)$ between the pair model calculation and the experimental value for both models of the pair interaction. It is clear that $\Delta_{\text{exp}}c(0)$

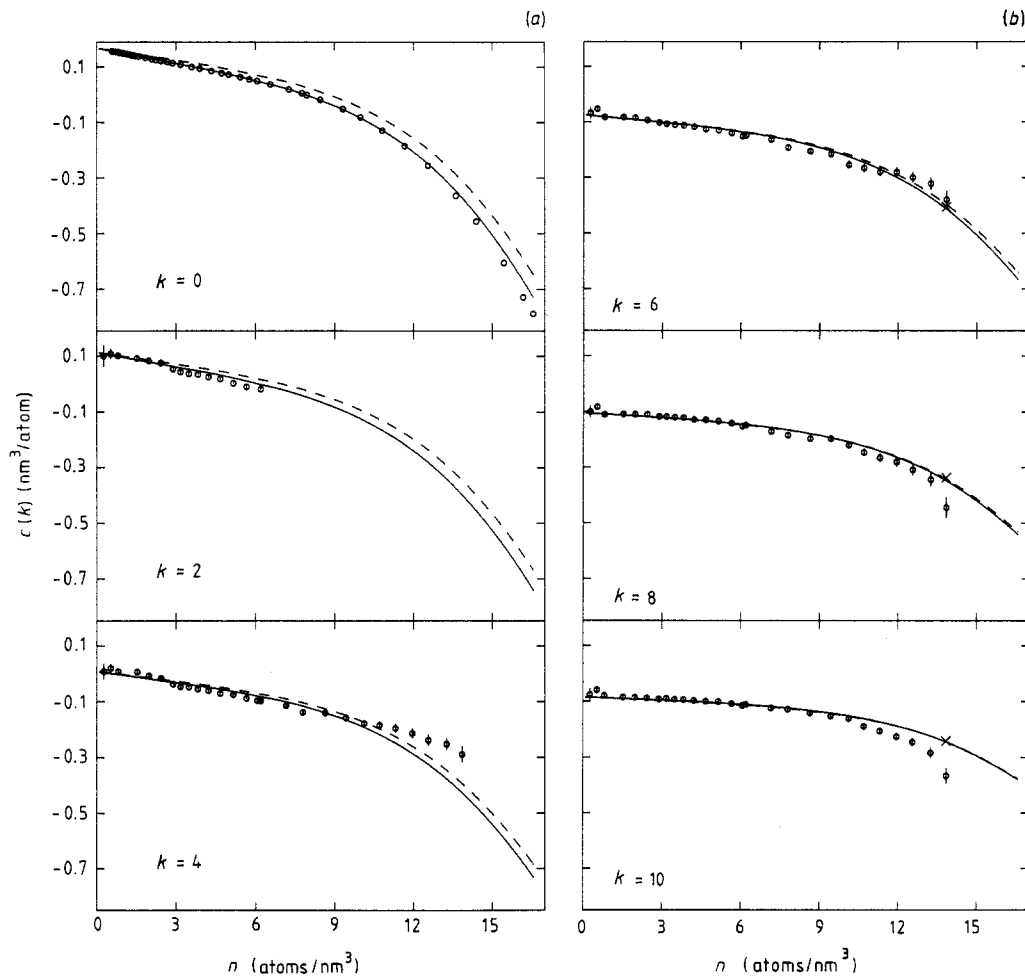


Figure 7. (a) Plots of $c(k)$ as a function of density at $k = 0, 2$ and 4 nm^{-1} for krypton at $T = 297 \text{ K}$: experiment (O); optimised CRS-MHNC for Barker u_2 (---) and for Barker plus DDD (—). (b) As in (a) at $k = 6, 8$ and 10 nm^{-1} . In addition: simulation result (Levesque and Weis 1988) at one density for HFGKR pair potential (Aziz 1979) plus DDD (x).

for the Aziz potential does not extrapolate to zero at $k = 0$ and this is a reflection of the discrepancy between the second virial coefficient of the Aziz potential and the value implied by the equation of state we are using, as discussed in the previous section. This explains the almost constant shift between $\Delta_{\text{exp}}c(0)$ for Aziz and for Barker up to a density of about 6 atoms/nm^3 . The discrepancy between the low-density behaviour of the experimental data we are using and virial coefficient measurements is small but significant for our purpose. In any case we can say that there is clear evidence for the presence of many-body forces that are repulsive on average. Up to a density of order of 10 atoms/nm^3 the triple dipole interaction gives a reasonable description of the compressibility of the system but the discrepancies are increased when the higher-order multipole terms are added. In this respect it is interesting to notice that $\Delta_{\text{exp}}c(0)$ shows oscillations around $\Delta_{\text{th}}c(0)$ in the density range $0\text{--}10 \text{ atoms/nm}^3$. This has an interesting

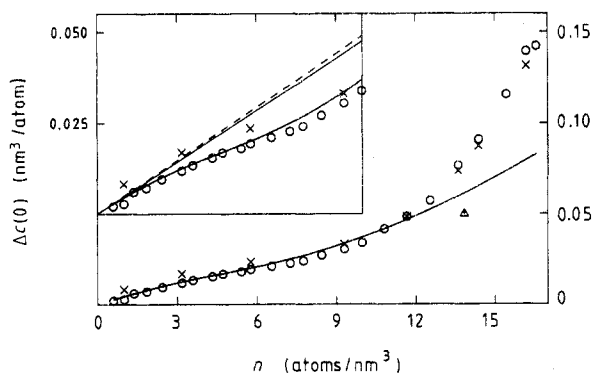


Figure 8. Difference $\Delta c(0) = c^{(2)}(0) - c^{(3)}(0)$ between the optimised CRS-MHNC $c(0)$ for the two-body model interaction and the two- plus three-body model (Barker u_2): DDD model (—) and Loubeyre model with increased strength as in figure 5 (Δ). In the inset the virial expansion results are also shown as straight lines; DDD model (—) and DDD + DDQ + DQQ + QQQ model (---). Additional symbols represent the difference between the pair model result and experiment (Trappeniers *et al* 1966): Barker u_2 (O) and Aziz u_2 (X).

Table 4. Coefficients of the best fit of $c(0)$ with equation (25). Theoretical results are from the CRS-MHNC equation for the indicated interactions and experimental result is deduced from Trappeniers *et al* (1966) as discussed in the text.

	α (nm ³ /atom)	$\beta \times 10^2$ (nm ⁶ /atom ²)	$\gamma \times 10^4$ (nm ⁹ /atom ³)
Barker	0.1680	-1.368	-3.48
Barker + DDD	0.1678	-1.813	-1.69
Experiment	0.1683	-1.930	+0.73

origin; it is due to the fact that the linear range in density is much larger for the experimental data than for any of the theoretical results. We have fitted the experimental and the theoretical data for $c(0)$ up to $n = 3$ atoms/nm³ with a quadratic form in density

$$c(0) = \alpha + \beta n + \gamma n^2 \quad (25)$$

and the resulting coefficients are given in table 4. If in this density range the terms of higher order in n give a negligible contribution one should find that $\alpha = c_0(0)$, $\beta = c_1^{(2)}(0)$ when the pair interaction is used and $\beta = c_1(0)$ when also $u^{(3)}$ is used. One notices only small deviations from these equalities and we conclude that this density range is adequate to assume that the value of γ gives an estimation of $c_2(0)$. It can be noticed that the three-body interaction decreases the value of $|\gamma|$ by more than a factor of 2 but the experimental value is significantly smaller and of opposite sign, again pointing to stronger many-body forces. The noise of the data leaves a rather large uncertainty on the value of γ and new data would be useful.

The deviation between $\Delta_{\text{th}}c(0)$ and $\Delta_{\text{exp}}c(0)$ increases rapidly with density above 10 atoms/nm³ and this deviation is much larger than the difference between the Barker and Aziz results. We have evidence that this deviation is not due to the multipolar terms beyond the DDD interaction. The DDQ, DQQ and QQQ interactions only give a small

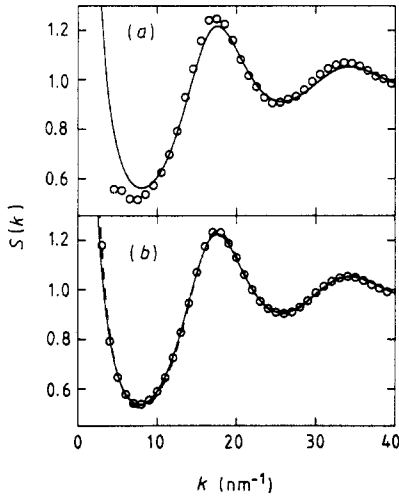


Figure 9. (a) The function $S(k)$ for krypton at $T = 220$ K and $n = 4.89$ atoms/nm³: experiment (Fredrikze 1987) (○) and theory as in figure 4. (b) Results at $T = 237$ K and $n = 5.582$ atoms/nm³: experiment from Youden (1987).

contribution at low density as already shown in figure 2 ($c_1^{(3)}(0)$ changes from 0.479×10^{-2} nm⁶/atoms² to 0.513×10^{-2} nm⁶/atoms² due to these multipolar terms). At larger density we have not performed a computation with CRS-MHNC with the full multipolar interaction but our computation at density 13.84 atoms/nm³ with the QQQ interaction allows us to estimate that the multipolar terms change $\Delta_{th}c(0)$ by only a few per cent. We conclude that at large density there is evidence for additional repulsive many-body forces.

We have plotted $\Delta_{exp}c(k)$ for the k -values shown in figure 7 and significant differences from $\Delta_{th}c(k)$ are found for all values of k . As can be seen from figure 7 these differences change sign between $k = 4$ and 10 \AA^{-1} . Again they indicate that additional short-ranged forces are needed.

4.3. The 200 K region

As an additional test of the models of the inter-atomic interaction we have computed $S(k)$ at some temperatures in the region of 200 K. The comparison with the Fredrikze (1987) data in the liquid phase at $T = 200$ K has already been presented (Reatto and Tau 1987) and here we present a comparison at higher T and lower density. The $S(k)$ at $T = 220$ K and $n = 4.89$ atoms/nm³ is shown in figure 9(a). Only the theoretical result, which includes the DDD interaction, is presented because this thermodynamic state is inside the spinodal line of the CRS-MHNC equation for the pure Aziz potential. At $k = 0$ (out of scale) the theoretical value $S(0) = 8.21$ is in reasonable agreement with the thermodynamic value (Fredrikze 1987) $S(0) = 7.54$. At finite k the deviation between experiment and theory is significant over all the measured k -range, there is both a shift and a different amplitude of the oscillations of $S(k)$ and the experimental $S(k)$ lies well below the theoretical one for $k < 10 \text{ nm}^{-1}$. However the k -scale used by Fredrikze (1987) is not exact (Fredrikze 1988) and some of the differences shown are due to this error. We have checked the accuracy of the CRS-MHNC equation by performing a molecular dynamic computation and the agreement is satisfactory also in this case.

Finally we present in figure 9(b) a comparison with the data of Youden (1987) for a similar thermodynamic state, $T = 237$ K and $n = 5.582$ atoms/nm³. On this scale the

agreement is good and of the same kind as that for the room-temperature isotherm at intermediate density (figure 4(a)).

5. Discussion

We have used the low-density expansion of the correlation functions and a new integral equation to evaluate both the pair correlation function and the structure factor for systems of atoms interacting with both pair and many-body potentials. By comparison with computer simulation data the integral equation results were shown to be accurate to about 1%, up to densities about twice the critical density and for temperatures roughly in the range $0.7 \leq k_B T/\varepsilon \leq 1.5$. With this tool, comparisons between theoretical predictions and experimental data become possible from $k = 0$ to all experimental k -values and for the complete range of experimental densities. Consequently it was possible to test several models for many-body forces in this way, without generating excessive demands for computer time. This is one of the first computations with the integral equation method in which realistic models of the inter-atomic forces have been used in a dielectric fluid, and this is because we are now able to take into account also the three-body interaction with high accuracy. The very wide region of thermodynamic states in which the CRS-MHNC equation (including three-body forces) is accurate allows a severe test of any model of the inter-atomic forces in a monatomic fluid.

In the low-density regime at room temperature our findings confirm previous evidence (Teitsma and Egelstaff 1980) for the presence of many-body forces in krypton. The multipolar expression for the three-body interaction gives a satisfactory representation of the thermodynamic value for $c(0)$ but deviations are found in $c(k)$ at finite k . Loubeyre's model for u_3 makes the results worse at both finite k and $k = 0$. Some subtle deviations in the compressibility data are found between experiment and the multipolar model. This suggests that additional many-body forces are present but some inconsistency between different equation-of-state data at low density points out that we need additional experimental data. Our results also indicate that in the search for signatures of many-body forces it is preferable to analyse the data in terms of $c(k)$ and not of $H(k)$. This is because the dependence of $c(k)$ on the detailed shape of u_2 is mainly contained in its low-density limit $c_0(k)$ but this is not so for $H(k)$. With respect to the pair potential we can say that the Barker and the Aziz u_2 give very similar results for $c(k)$ at finite k , the deviations being well below the present experimental accuracy. Some deviations between the two $c(k)$ are only found at small k and at $k = 0$ the Barker u_2 is in better agreement with the experimental data (Trappeniers *et al* 1966, Michels *et al* 1960) we have used. However, we cannot draw a conclusion from this in view of the fact that the Aziz u_2 is in good agreement with some other experiments (Aziz 1979).

When we consider a wider density range, say up to 10 atoms/nm³, we find substantial agreement between experiment and theory but here the evidence for three-body effects is limited because the effect of u_3 on $c(k)$ is small. Nevertheless the plots of $\Delta c(k)$ for experiment and theory show differences which require three-body terms beyond the multipolar series. Above this density, theory and experiment start to diverge. The deviations increase very strongly with density and are present at all k , $k = 0$ included. This is a signature for additional many-body forces. None of the models for u_3 we have considered improves the situation. The $k = 0$ result indicates that these additional many-body forces are repulsive on average and this is in disagreement with Loubeyre's model for u_3 . In addition these short-range many-body forces should have a comparatively

stronger effect than the triple dipole one on the structure of the system and this can only be obtained if the angular dependence of u_3 at short distance differs from the triple dipole one. The other possibility is that fourth- and higher-order many-body interactions become important at high density. It is possible that these two options could be distinguished experimentally by high-precision measurements as a function of density.

It is evident that this is a time-consuming, sophisticated field, and that a proper understanding of even the simplest fluid will be impossible without a reasonably detailed treatment of many-body forces. This should not be surprising because atomic polarisability plays such an important role in the treatment of pair forces. We hope that this paper has demonstrated new, and perhaps successful, methods for addressing this problem.

Acknowledgments

The work of two of us (LR and MT) has been supported in part by Centro Interuniversitario Struttura della Materia del Ministero Pubblica Istruzione and by Consiglio Nazionale Ricerche under the Italia–US Cooperative Science Program. The work of PAE was supported by the Natural Sciences and Engineering Research Council of Canada.

References

- Axilrod B M and Teller E 1943 *J. Chem. Phys.* **11** 299
Aziz R 1979 *Mol. Phys.* **38** 177
Aziz R, Mathur K and Slaman M J 1986 *Mol. Phys.* **58** 679
Barker J A 1986 *Mol. Phys.* **57** 755
Barker J A, Watts R O, Lee J K, Shafer T P and Lee Y T 1974 *J. Chem. Phys.* **61** 308
Bell R J 1970 *J. Phys. B: At. Mol. Phys.* **3** 751
Bulski M and Chalasinski G 1987 *J. Chem. Phys.* **86** 937
Celi S, Reatto L and Tau M 1989 *Phys. Rev. A* **39** 1566
Doran M B and Zucker I J 1971 *J. Phys. C: Solid State Phys.* **4** 307
Egelstaff P A, Gläser W, Litchinsky D, Schneider E and Suck J B 1983 *Phys. Rev. A* **27** 1106
Egelstaff P A, Teitsma A and Wang S S 1980 *Phys. Rev. A* **22** 1702
Foiles S M, Ashcroft N H and Reatto L 1984 *J. Chem. Phys.* **80** 4441
Fredrikze H 1987 *Phys. Rev. A* **36** 2272
——— 1988 private communication
Henderson D and Grundke E W 1975 *J. Chem. Phys.* **63** 601
Lado F 1982 *Phys. Lett.* **89A** 196
Levesque D and Weis J J 1988 *Phys. Rev. A* **37** 3967
Loubeyre P 1987 *Phys. Rev. Lett.* **58** 1857
Michels A, Levelt J M and deGraaff W 1960 *Physica* **26** 649
Muto Y 1943 *Proc. Phys. Math. Soc. Japan* **17** 629
Patey G N and Valleur J P 1976 *J. Chem. Phys.* **64** 170
Ram J, Barker R, Cummings P T and Egelstaff P A 1982 *Phys. Chem. Liq.* **11** 315
Ram J and Egelstaff P A 1984 *Phys. Chem. Liq.* **14** 29
Reatto L and Tau M 1987 *J. Chem. Phys.* **86** 6174
Rice S A and Gray P 1976 *Statistical Mechanics of Simple Liquids* (New York: Wiley)
Teitsma A and Egelstaff P A 1980 *Phys. Rev. A* **21** 367
Trappeniers N J, Wassenaar T and Wolkers G J 1966 *Physica* **32** 1503
Verlet L and Weis J J 1972 *Phys. Rev. A* **5** 939
Youden J A 1987 *MSc Thesis Guelph*